



20th EURO Working Group on Transportation Meeting, EWGT 2017, 4-6 September 2017,
Budapest, Hungary

Notes on Using Simulation-Optimization Techniques in Traffic Simulation

Xavier Ros-Roca^a, Lúdia Montero^b and Jaume Barceló^{b*}

^a *Accenture Analytics, Barcelona 08022, Spain*

^b *Universitat Politècnica de Catalunya, Barcelona 08034, Spain*

Abstract

Mathematical and simulation models of systems lay at the core of many decision support systems, and their role becomes more critical when the system is more complex. The decision process usually involves optimizing some utility function that evaluates the performance indicators measuring the impacts of the decisions. The complexity of the system directly increases the difficulty when the associated function to be optimized is a non-analytical, non-differentiable, non-linear function that can only be evaluated by simulation. Simulation-optimization techniques are especially suited to these cases, and its use is becoming increasingly used with traffic models, which represent an archetypal case of complex, dynamic systems that exhibit highly stochastic characteristics. In this approach, simulation is used to evaluate the objective function, and it is combined with a non-differentiable optimization technique for solving the associated optimization problem. Of these techniques, one of the most commonly used is Stochastic Perturbation Stochastic Approximation (SPSA).

This paper analyses, discusses and presents the computational results from applying this technique in the calibration of traffic simulation models. This study uses variants of the SPSA by replacing the usual gradient approach with a combination of projected gradient and trust region methods. A special approach has also been analyzed for parameter calibration cases in which each variable has a different magnitude.

© 2017 The Authors. Published by Elsevier B.V.

Peer-review under responsibility of the scientific committee of the 20th EURO Working Group on Transportation Meeting.

Keywords: Simulation-optimization; Traffic Simulation; Calibration of Simulation Models; Simultaneous Perturbation Stochastic Approximation

* Corresponding author. Tel.: +93-401-7033.

E-mail address: jaume.barcelo@upc.edu

1. Introduction

Modeling techniques aim to represent systems in terms of formal descriptions that are suitable for computer implementation with a variety of objectives that range from gaining a better theoretical understanding of a system's nature and operations, to their practical use as engines of Decision Support Systems, to helping operators make more rational decisions for analyzed systems.

As a representation of reality, a model is a simplified approximation of that reality, i.e., the system being modeled. Thus, using the model immediately raises questions about the validity and reliability of the decisions it supports. Box's assertion that "all models are wrong" is quite frequently quoted, yet the second part of that quote is more frequently forgotten, namely: "but some are useful". The correct use of a model therefore implies posing the question "What makes a model useful?" This question can be answered in terms of model calibration. Models are usually formulated in terms of parameters whose value must be estimated. Calibration can be defined as the process of estimating the most appropriate values of the parameters that will allow the model to accurately reproduce the studied system. The calibration problem can be formulated, (Rouphail and Sacks, 2003) in terms of finding the parameter values that reduce the probable distance between "reality" and the *model prediction* to less than d – which is a tolerable expression of the model's proximity to reality – and that the level of assurance is greater than a – that is, the index of significance for how certain we are. Stating it in mathematical terms:

$$P\{|reality - model\ prediction| < d\} > a \quad (1)$$

Assuming that the knowledge about "reality" is expressed in terms of the measured values of a set \mathcal{R} of observable variables, and that the prediction of the model M is expressed in terms of the estimated values of these variables, $\mathcal{S}(\mathbf{P})$, which are a function of the set of model parameters $\mathbf{P} = \{p_1, \dots, p_N\}$ whose values have to be calibrated, the formal definition of calibration can be re-stated in terms of the optimization problem:

$$\begin{cases} \min & \mathcal{F}[\mathcal{R}, \mathcal{S}(\mathbf{P})] \\ \text{s. t.} & \mathbf{P} \in \Omega \subseteq \mathbb{R}^N \end{cases} \quad (2)$$

where $\mathcal{F}[\mathcal{R}, \mathcal{S}(\mathbf{P})]$ is an error, i.e., a distance function between real observations; \mathcal{R} and \mathcal{S} are the corresponding simulated data; and Ω is the open set of \mathbb{R}^N in which the parameter values are feasible. The resulting optimization problem is non-convex and non-linear, and the function $\mathcal{F}[\mathcal{R}, \mathcal{S}(\mathbf{P})]$ cannot be represented analytically as a function of the parameters $\mathbf{P} = \{p_1, \dots, p_N\}$. Therefore, it is non-differentiable with respect to the parameters. Furthermore, the function $\mathcal{F}[\mathcal{R}, \mathcal{S}(\mathbf{P})]$ cannot be computed analytically and, consequently, it must usually be numerically evaluated by simulation, which makes the problem a natural candidate for simulation-based optimization methods (Osorio and Chong, 2015). This prompts resorting to non-differentiable optimization methods such as SNOBFIT, Genetic Algorithms, SPSA and others. This paper uses the optimization procedure SPSA, which was originally designed (Spall, 1998a) to solve the non-differentiable simulation-based optimization problems that are typical in simulation applications. It is therefore a natural candidate for solving problem (2). SPSA is even more appealing than other candidates since all non-differentiable methods strongly rely on evaluations of the objective function, which are computationally expensive in simulations, and SPSA requires fewer evaluations than other approaches.

2. Calibration and Validation of Traffic Simulation Models

The most currently used conventional methodological approach is FHWA (2004), which splits the calibration process into two major steps:

- Calibration of the supply
- Calibration of the demand

Very recent trends propose new approaches (Lu et al, 2015) that consider calibration as a single process for calibrating supply and demand simultaneously. However, in certain cases such as linear structures, the calibration of

the supply becomes the main concern. Such would be the case for freeways and motorways, where route choice is not an issue because for each entry ramp there is only one path to every exit ramp, with each route being unique. This is the case addressed in this paper. Calibrating the supply is namely a problem of finding the appropriate values for both the car-following and lane-changing parameters. Car-following models aim to reproduce traffic flows by reproducing the dynamics of car pairs (i.e., leaders and followers) and describing how each follower adapts its behavior to changes in its leader's behavior. In essence a car-following model is composed of a binomial: a mechanical entity, the car (with certain physical characteristics, e.g., maximum acceleration/deceleration capabilities, vehicle length, etc.); and a human driver whose behavioral characteristics are described by parameters such as desired speed, minimum headway, sensitivity to a stimulus, etc. From a formal point of view, car-following models can be formulated as instances of a follower's acceleration law, (Wilson and Ward, 2010):

$$a_{n+1}(t) = f[s_{n+1}(t), \Delta v_{n+1}(t), v_{n+1}(t)] \quad (3)$$

in which the response of the following vehicle $n + 1$ at time t is defined in terms of its acceleration $a_{n+1}(t)$ as a function of $s_{n+1}(t)$, the spacing between the lead vehicle n and the following vehicle $n + 1$ at time t , the relative speed between follower and leader $\Delta v_{n+1}(t)$ at time t , and the current speed of the follower $v_{n+1}(t)$ at time t . A wide variety of car-following models can be derived, depending on the postulated form of the function $f[\cdot]$.

In our work, we consider the function resulting from the safety-to-stop distance modeling hypothesis (Gerlough and Huber, 1975), which leads to the deceleration component of Gipps model (Gipps 1981), whose acceleration component is based on an empirical analysis of recorded data:

$$v_{n+1}(t + \tau) = \min \left\{ \begin{array}{l} v_{n+1}(t) + 2.5a_{n+1}\tau \left(1 - \frac{v_{n+1}(t)}{V_{n+1}} \sqrt{0.025 + \frac{v_{n+1}(t)}{V_{n+1}}} \right) \\ b_{n+1}\tau + \sqrt{(b_{n+1}\tau)^2 - b_{n+1} \left(2(x_n(t) - s_n - x_{n+1}(t)) - v_{n+1}(t)\tau - \frac{v_n(t)^2}{\hat{b}} \right)} \end{array} \right. \quad (4)$$

where a_{n+1} , b_{n+1} are the maximum acceleration and braking (m/s^2) that the driver of the following vehicle can apply, \hat{b} is the estimated maximum braking that the lead vehicle applies, $s_n = L_n + \Delta_n$ is the "safety distance" (the length of the lead vehicle L_n plus a safety gap Δ_n), V_{n+1} is the maximum desired speed of the follower, and $x_{n+1}(t)$, $x_n(t)$, $v_{n+1}(t)$, $v_n(t)$ are, respectively, the current locations and speeds of follower and leader at time t .

To avoid vehicles in the simulation model becoming behaviorally identical, the car-following models usually implemented in all simulation software assumes that the parameters describing the driver population have random variations, which are described by the probability distributions from which they are sampled. Taking this into account, the parameters chosen for the calibration exercise are:

- 1) **Maximum Desired Speed (Mean)**: The maximum speed applied to a vehicle class that models a driver type where no speed restriction is active in sections along the path, because either the speed limit is over the desired speed or no congestion effects are present. This is measured in km/h.
- 2) **Maximum Desired Speed (Standard Deviation)**: The Standard Deviation of the Maximum Desired Speed distribution. Measured in km/h.
- 3) **Speed Acceptance (Mean)**: This quantifies how much the driver accepts the speed limit of the road. It is a non-negative parameter around 1 with the following values: below 1 means that she or he will obey the limits while above 1 means the driver will not respect the limit. It is a dimensionless measure.
- 4) **Speed Acceptance (Standard Deviation)**: The Standard Deviation of the Speed Acceptance distribution.
- 5) **Clearance (Mean)**: The distance a vehicle maintains between itself and the preceding vehicle when stopped. It is measured in meters.
- 6) **Clearance (Standard Deviation)**: The Standard Deviation of the Clearance distribution. Measured in meters.
- 7) **Reaction Time**: The time it takes a driver to react to the speed changes of the preceding vehicle. Measured in seconds.
- 8) **Reaction Time at Stop**: The time it takes a stopped vehicle to react to the acceleration of the vehicle in front.

- 9) **Margin for Overtaking Maneuver (Mean):** The safety time gap between the overtaking car and the oncoming car. Measured in seconds.
- 10) **Margin for Overtaking Maneuver (Standard Deviation):** The Standard Deviation of the Margin for Overtaking Maneuver distribution. Measured in seconds.
- 11) **Gap (Mean):** The distance between the follower and the leader. Measured in meters.
- 12) **Gap (Standard Deviation):** The Standard Deviation of the Gap distribution. Measured in meters.

The objective function $\mathcal{F}[\mathcal{R}, \mathcal{S}(\mathbf{P})]$ in our calibration process is formulated in terms of the traffic variables measured at the test site, which are obtained from the radar and Bluetooth antenna technologies equipping the site:

- **Flow: (veh/h)** The number of vehicles crossing the radar sensor per hour.
- **Speed: (km/h)** The average speed of the vehicles crossing the radar sensor.
- **Travel Time: (seconds)** The average time needed for a sample of vehicles to travel between two Bluetooth antennas.

$$\mathcal{F}[\mathcal{R}, \mathcal{S}(\mathbf{P})] = f_q(q_{1,\tau_1}, \dots, q_{n_R,\tau_T}; \hat{q}_{1,\tau_1}, \dots, \hat{q}_{n_R,\tau_T}) + f_v(v_{1,\tau_1}, \dots, v_{n_R,\tau_T}; \hat{v}_{1,\tau_1}, \dots, \hat{v}_{n_R,\tau_T}) + f_t(t_{1,\tau_1}, \dots, t_{n_B,\tau_T}; \hat{t}_{1,\tau_1}, \dots, \hat{t}_{n_B,\tau_T}) \quad (5)$$

Where $q_{i,\tau_j}, v_{i,\tau_j}, \forall i = 1, \dots, n_R, j = 1, \dots, T$ stand for measured flows and speeds for each of the n_R radar stations and T time intervals, and $t_{i,\tau_j}, \forall i = 1, \dots, n_B, j = 1, \dots, T$ for measured travel times between each of the n_B pairs of Bluetooth antennas for each time interval. The same notation with “hats” denotes the corresponding simulated values. To avoid possible scale effects arising from each term of the objective function (5) corresponding to a different magnitude and measurement unit, the terms in the formulation of (5) are expressed as *Normalized Root Mean Square Errors* (NRMSE), defined as:

$$NRMSE(\mathbf{x}, \hat{\mathbf{x}}) = \frac{\sqrt{\frac{\sum_{i=1}^n (x_i - \hat{x}_i)^2}{n}}}{\max(x) - \min(x)}$$

Then the normalized error function in optimization problem (2), in terms of flows \mathbf{q} , speeds \mathbf{v} and travel times \mathbf{t} , is:

$$\mathcal{F}[\mathcal{R}, \mathcal{S}(\mathbf{P})] = NRMSE(\mathbf{q}, \hat{\mathbf{q}}) + NRMSE(\mathbf{v}, \hat{\mathbf{v}}) + NRMSE(\mathbf{t}, \hat{\mathbf{t}})$$

3. Site Description

The selected site is a nearly 7.5 km section of a Swedish highway, which connects Stockholm with its most important airport, Arlanda. The selected section is near the city of Solna, to the north of the Swedish capital, and it is intensively used daily by downtown workers commuting from the outskirts of Stockholm. This site was chosen first because it is an important section of the highway serving as one of the main entrances to Stockholm and, second, because it is adequately equipped with a sensor network that provides a large amount of data, which is essential for calibrating a simulated model. The network consists of 12 Radar and 8 Bluetooth sensors that are well distributed along the studied section and which provided measures of flows, average speeds and travel times during March, April and May 2015, aggregated to five-minute intervals.

The selected site runs nearly straight throughout and ends at the entrance of a tunnel, where it turns significantly to the right. This 7.5 km section alternates between 3 and 4 lanes, with 5 entry lanes and 3 exit lanes where vehicles can get on or off the highway, respectively. A microscopic model of the described site was built in July 2015 and was used in this work. The site traffic simulation model was built with Aimsun, whose traffic demand inputs were defined in terms of input flows at entry ramps and turning proportions at exit ramps. Aimsun provides default values for the behavioral parameters defined above; thus, the calibration process consists of finding suitable values for the site.

4. SPSA and Innovations

Spall (1998a) presents a basic implementation of the *Simultaneous Perturbation Stochastic Approximation* (SPSA) algorithm, which is an iterative algorithm for minimizing problems such as (2) while actually running fewer evaluations of the cost function. The SPSA procedure is a recursive method which starts with an initial combination of parameter values $\mathbf{P}_0 = (p_1^0, \dots, p_N^0)$, with the next points being generated by:

$$\mathbf{P}_{k+1} = \mathbf{P}_k - a_k \cdot \hat{\mathbf{g}}_k(\mathbf{P}_k) \quad (6)$$

where a_k is a decreasing sequence of positive numbers and $\hat{\mathbf{g}}_k(\mathbf{P}_k)$ is the approximation to the gradient. This gradient approximation in (6) is a variation of the finite differences method, which requires only 2 evaluations of the cost function:

$$\hat{\mathbf{g}}_k(\mathbf{P}_k) = \frac{\mathcal{F}[\mathcal{R}, \mathcal{S}(\mathbf{P}_k + c_k \cdot \Delta_k)] - \mathcal{F}[\mathcal{R}, \mathcal{S}(\mathbf{P}_k - c_k \cdot \Delta_k)]}{2c_k} \cdot \Delta_k^{-1}$$

where c_k is another decreasing sequence of positive numbers and $\Delta_k \in \mathbb{R}^N$ is a vector of independent and identically distributed random variables with certain properties fully described in Spall (1998a). Typically used sequences are $a_k = a/(A + k + 1)^\alpha$, $c_k = c/(k + 1)^\nu$ and $\Delta \sim Be(1/2, \pm 1, N)$, which stands for an N -dimensional i.i.d. Bernoulli vector of ± 1 with probability $1/2$. The parameters in the algorithm are adjusted by following the procedure described in Spall (1998b). The classical means for incorporating the Trust Region of feasible values for the problem in (2) is to orthogonally project the parameter vector onto the boundary of $\Omega \subset \mathbb{R}^N$ in cases where vector $\mathbf{P} \notin \Omega$. In calibration problems, Trust Region is usually a Cartesian product of intervals, $\Omega = [a_1, b_1] \times \dots \times [a_N, b_N]$, which are the feasibility limits of the parameters. Note that this procedure updates all the parameters by subtracting the same value from all the parameters, due to the way in which the gradient approximation is computed with only two evaluations. This could be a drawback in calibration problems with different magnitude parameters – as in the case presented in this work – because large magnitude parameters vary slightly after the update while other parameters of lower magnitude can oscillate widely. In these cases, adjusting neither the method nor the parameters can solve it because it can lead to slow convergences.

Two different solutions to this problem are proposed in this work. The first solution relies on the fact that the Trust Region is a rectangle of \mathbb{R}^N and can be transformed into a cube of the same space by normalizing the magnitude of all the parameters. The second solution is inspired by Wang et al. (2008) and consists of keeping the problem free from constraints and adding a penalty term to the cost function.

4.1. Normalization of the parameters

The homogenization of the parameter magnitudes was done using linear interpolations such as:

$$\begin{aligned} \varphi_i: [a_i, b_i] &\rightarrow [0, 10] \\ p_i &\mapsto \tilde{p}_i = 10 \frac{p_i - a_i}{b_i - a_i} \end{aligned}$$

Therefore, letting $\Phi = (\varphi_1, \dots, \varphi_N)$ and its inverse be the correspondent functions from Ω to $\tilde{\Omega} = [0, 10]^N$, the problem (2) can be written as

$$\begin{cases} \min & \tilde{\mathcal{F}}[\mathcal{R}, \mathcal{S}(\tilde{\mathbf{P}})] \\ \text{s. to} & \tilde{\mathbf{P}} \in \tilde{\Omega} = [0, 10]^N \end{cases} \quad (7)$$

Where $\tilde{\mathcal{F}}[\mathcal{R}, \mathcal{S}(\tilde{\mathbf{P}})] = \mathcal{F} \circ \Phi$ and the minimum of problem (7), $\tilde{\mathbf{P}}^*$, can be translated to the minimum of problem (2) by undoing the transformation, that is $\mathbf{P}^* = \Phi(\tilde{\mathbf{P}}^*)$. In problem (7), the changes affect each parameter proportionally to its magnitude.

4.2. Penalized Objective Function

The alternative penalty-function approach consists of transforming the constrained minimizing problem to a free minimizing problem by modifying the objective function in a more formal way:

$$\begin{cases} \min & \mathcal{F}[\mathcal{R}, \mathcal{S}(\mathbf{P})] + r \cdot P(\mathbf{P}) \\ \text{s. to} & \mathbf{P} \in \mathbb{R}^N \end{cases} \quad (8)$$

where $P(\mathbf{P}) \geq 0$ is a penalty function that penalizes those $x < \Omega$, and r is a positive real number such that the minimum of the new problem (8) is the same as in the original problem (2). The penalty functions are functions that increase the objective cost when the parameters do not belong to the Trust Region. Defining the set $\Omega := \{q_j(\mathbf{P}) \leq 0\}$ as a set of constraints, $P(\mathbf{P})$ is usually chosen as a different function different to 0 if and only if $q_j(\mathbf{P}) > 0$ for any one of the constraints. In this paper, a quadratic penalization is chosen, that is $P(\mathbf{P}) = \sum_j \alpha_j \cdot \max\{q_j(\mathbf{P}), 0\}^2$, where α_j are factors for adjusting the importance of each constraint. In this second incorporation, the step of the recursive method described in (6) is modified by adding the corresponding derivative of the penalizing function:

$$\nabla[\mathcal{F}(\mathbf{P}) + r \cdot P(\mathbf{P})] = \nabla\mathcal{F}(\mathbf{P}) + r \cdot \nabla P(\mathbf{P}) = \nabla\mathcal{F}(\mathbf{P}) + r \sum_j \alpha_j \cdot \max\{q_j(\mathbf{P}), 0\} \cdot \nabla q_j(\mathbf{P})$$

Therefore, the parameters of our SPSA proposal evolve iteration by iteration using the following iterative equation, where $r_k = r/k^{0.1}$, as proposed in Wang et al. (2008).

$$\mathbf{P}_{k+1} = \mathbf{P}_k - a_k \{ \hat{\mathbf{g}}_k(\mathbf{P}_k) + r_k \sum_j \alpha_j \cdot \max\{q_j(\mathbf{P}_k), 0\} \cdot \nabla q_j(\mathbf{P}_k) \} \quad (9)$$

5. Experimental Results

The results of this work were obtained by combining both proposals described in Section 4, first by normalizing parameters and then using the penalized SPSA. The 12 behavioral parameters for the model of the described site were calibrated using the values for the SPSA algorithm parameters: $a = 2.2$, $c = 0.6$, $A = 6$, $r = 1$ and $\alpha = 0.602$, $\gamma = 0.101$, following the parameter lines of Spall (1998b).

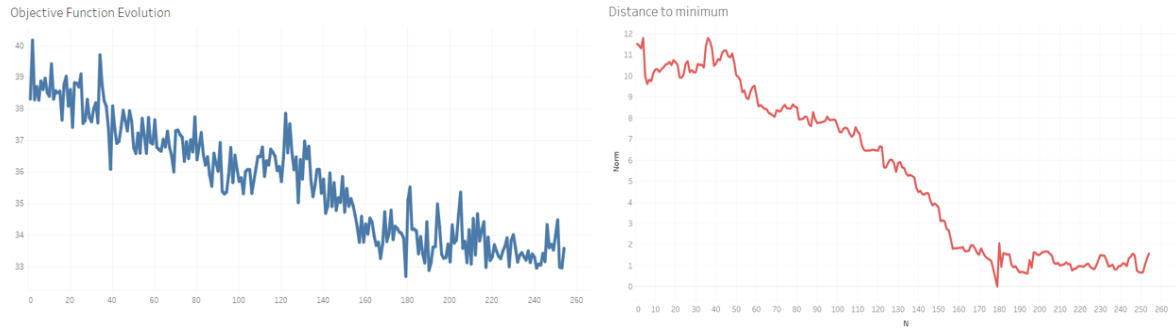


Fig. 1. (a) Objective function evolution of SPSA performance; (b) $\|\tilde{\mathbf{P}}_k - \tilde{\mathbf{P}}^*\|_2$ evolution.

The real observed data selected for the calibration was a subset of 1 hour on 19 March 2015, from 10:30AM to 11:30AM, aggregated at the 5minute level for computational reasons. The algorithm stopped after 254 iterations, using as stopping criteria the relative differences between consecutive iterations of less than 10^{-6} . Figure (1a) shows the evolution of the cost function while progressing to the solution. Note that it decreases while reaching the minimum at iteration 179, denoted by $\tilde{\mathbf{P}}^*$. Then, the sequence remains oscillating around the neighborhood of this local optimum oscillating, as can be seen in Figure (1b), where the Euclidean distance is plotted between the minimum $\tilde{\mathbf{P}}^*$ and the vector of parameters at each iteration, $\tilde{\mathbf{P}}_k$.

Table 1. Results of the Calibration Procedure.

Behavioral Parameters	Values [units]
Max. Desired Speed (Mean, Std Dev)	(102.173, 8.540) [km/h]
Speed Acceptance (Mean, Std Dev)	(0.688, 0.329) [u]
Clearance (Mean, Std Dev)	(1.368, 0.474) [m]
Reaction Time	1.077 [s]
Reaction Time at Stop	1.133 [s]
Margin for Overtaking Man. (Mean, Std Dev)	(5.530, 3.491) [s]
Gap (Mean, Std Dev)	(0.584, 0.247) [m]



Fig. 2. Top: Simulated vs. Real in Calibration dataset (a) Flows; (b) Speeds; (c) Travel Times. Below: Simulated vs. Real in Validation dataset (a) Flows; (b) Speeds; (c) Travel Times

The estimated parameters that converge at iteration 179 are in Table 8.1. These values are accepted as the optimal values for reaching the minimum objective function, which is denoted as $\mathbf{P}^* = \Phi^{-1}(\hat{\mathbf{P}}^*)$. A quick analysis of these parameters shows the particularities of Swedish drivers on a highway. For instance, notice they completely accept speed limits of 90 km/h and their maximum desired speed is around 100 km/h. Both Reaction Time and Reaction Time at Stop are quite similar, which is coherent with the fact that the site is a highway with no severe congestion present during the simulated interval and there are no flow interruptions from signalized intersections, as occurs in urban networks.

5.1. Calibration and Validation Results

Figure (2-top) shows the comparison of observed and simulated data at convergence for the calibration dataset (colors indicate different measuring objects, and shapes different time intervals within the contemplated period). Figure (2-below) shows the same graphics for the validation dataset. The correlation between the three measures and their corresponding simulated values is very high. Note in Figure (2a-top) that the flow measure has a significant bias – because the model is simulating fewer vehicles – and that discrepancies between the flow values increase remarkably as one moves forward in the section. Figure (2a-top) depicts two clear clusters for section flows: the first belongs to exit lanes (bottom-left area) and shows low flows; while the second cluster contains the main sections where observed flows are slightly greater than simulated flows, thus leading to simulated speeds that are greater than those that were observed, as can be seen in Figure (2b-top). NRMSE for flow, speed and travel times is about 0.11, and overall Theil coefficients are less than 0.05 for speeds and travel times but close to 0.09 for flows in the calibration dataset. Validation results are only slightly worse. Flow, speed and travel times also fit satisfactorily to the validation dataset in Figure (2-below).

6. Conclusions and Future Research

The results of this work suggest that SPSA-based calibration of microscopic traffic models is promising and should be extended to assisting users in the simultaneous short-term calibration of microscopic car-following and route-choice parameters for network models. Further research will investigate the application of the procedure to other car-following models and further study the effect of congestion on the stability and convergence of the proposed procedure. An extended line of research could consider time-series models that would actually aim at predicting the evolution of these parameters in discrete time-sliced intervals. Correlation between parameters can also be considered in future research or heterogeneity of behavior according to driver segmentation based on knowledge of the network and of the presence of an on-board navigation system. Finally, demand calibration for time-sliced Origin-Destination demand matrices could lead to extended suitable SPSA-based procedures for dealing with the simultaneous calibration of supply and demand, which is needed in non-linear models where several alternative paths are available for each OD pair.

Acknowledgments

This research was funded by TRA2016-76914-C3-1-P of the Spanish R+D National Programs and by the *Secretaria d'Universitats i Recerca de la Generalitat de Catalunya* under 2014 SGR 1534. We are grateful for the support of Rasmus Ringdahl and Joakim Ekstrom from Linköping University during the development of the work and for their providing access to the site's traffic data and Aimsun model.

References

- FHWA, 2004. *Traffic Analysis Toolbox, Volume II: Guidelines for Applying Traffic Microsimulation Software*. Publication FHWA-HRT-04-040, FHWA, U.S. Department of Transportation, http://ops.fhwa.dot.gov/trafficanalysis/tat_vol3.
- Gerlough, D.L., Huber, M.J., 1975. *Traffic Flow Theory: A Monograph*. TRB Special Report 165. Washington.
- Gipps, P.G., 1981. A behavioral car-following model for computer simulation. *Transp. Res. B, Vol. 15* pp 105-111.
- Lu, L., Xu, Y., Antoniou, C., Ben-Akiva, M., 2015. An enhanced SPSA algorithm for the calibration of Dynamic Traffic Assignment Methods. *Transportation Research C 51* pp.149-166.
- Osorio, C., Chong, L., 2015. A computationally efficient simulation-based optimization algorithm for large-scale urban transportation problems. *Urban Transportation Problems, 49* (33) pp 623–636.
- N. M. Roupail and J. Sacks, 2003. *Workshop on Modeling Trends*. Sitges
- Spall, J.C., 1998a. An overview of the simulation perturbation method for efficient optimization. *APL Technical Digest 19*(4) pp 482–492.
- Spall, J.C., 1998b. Implementation of the Simultaneous Perturbation Algorithm for Stochastic Optimization. *IEEE Trans. Aerosp. Electron. Syst.* 34(3), pp 817–823.
- Wilson, R. E., Ward, J. A., 2010. *Car-following models: fifty years of linear stability analysis, a mathematical perspective*. UTSG Plymouth.
- Wang, I.J, Spall, J.C., 2008. Stochastic Optimization with inequality constraints using simultaneous perturbations and penalty functions, *International Journal of Control 81*(8) pp 1232–1238.